

## Supporting Information

### Modulating packing and photovoltaic performance of (bisthiophene)benzene-linked polymer acceptors through simple methylation engineering

Ruiqi An,<sup>ab</sup> Mengqi Cao,<sup>ab</sup> Hongxiang Li,<sup>c</sup> Zhongxiang Peng,<sup>a</sup> Xiaofu Wu,<sup>\*a</sup> Hui Tong<sup>\*ab</sup> and Lixiang Wang<sup>\*ab</sup>

<sup>a</sup> State Key Laboratory of Polymer Physics and Chemistry, Changchun Institute of Applied Chemistry, Chinese Academy of Sciences, Changchun, 130022, China

<sup>b</sup> University of Science and Technology of China, Hefei, 230026, China

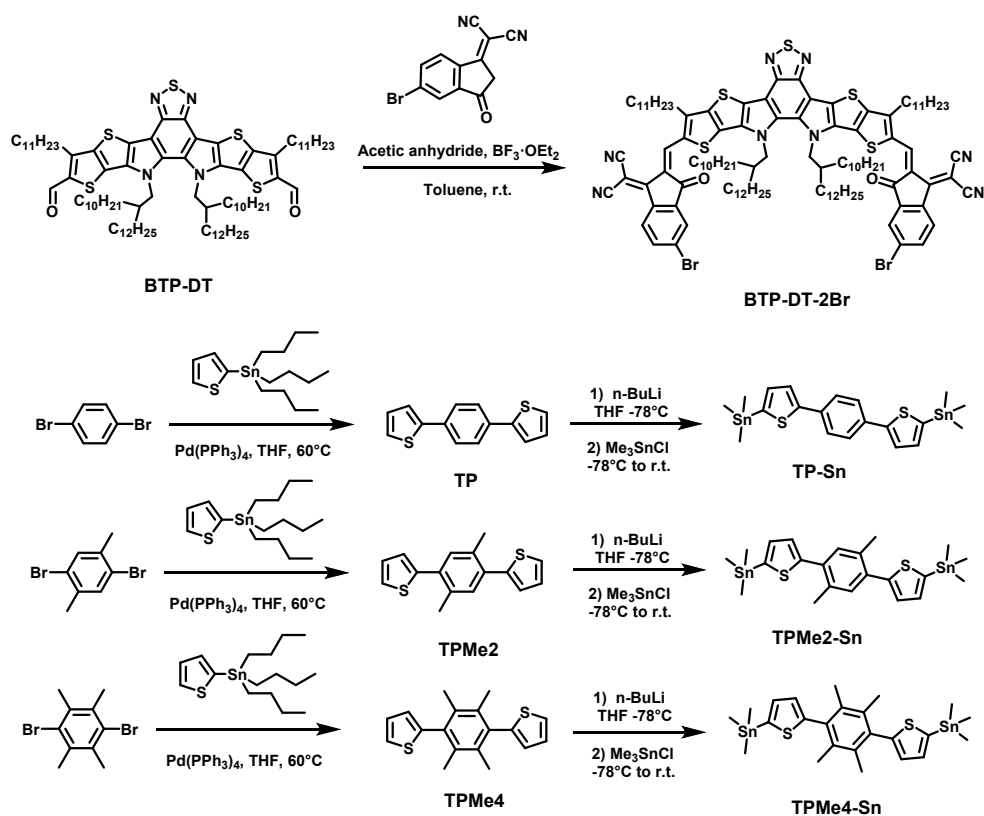
<sup>c</sup> College of Polymer Science and Engineering, State Key Laboratory of Polymer Materials Engineering, Sichuan University, Chengdu 610065, China

\* Corresponding author: [wxp@ciac.ac.cn](mailto:wxp@ciac.ac.cn); [chemtonghui@ciac.ac.cn](mailto:chemtonghui@ciac.ac.cn); [lixiang@ciac.ac.cn](mailto:lixiang@ciac.ac.cn)

## 1. Experimental section

### 1.1. Materials and synthesis

Solvents used in the synthesis were dried according to standard procedures. All raw materials and reagents that purchased from commercial sources were used directly without further purification. The polymer donor PM6 was purchased from Derthon Optoelectronic Materials Science Technology Co., Ltd, and the material BTP-DT was purchased from Zhengzhou Alfa Chemical Co., Ltd.



**Scheme S1** Synthetic routes of polymer monomers.

**Synthesis of TP.** 1,4-Dibromobenzene (1 g, 4.24 mmol) and 2-(tributylstannyl)thiophene (3.95 g, 10.60 mmol) were added into a 2-neck flask. After three gas exchanges under an argon atmosphere, tetrakis(triphenylphosphine)palladium (245 mg, 0.21 mmol) and Toluene (25 mL) were added to the flask. Then the reaction mixture was heated at  $100^\circ\text{C}$  overnight under argon. After cooling down the reaction

solution to room temperature, the mixture was concentrated and purified by column chromatography (silica, petroleum ether) afforded the title compound (819 mg, 80%) as a white solid.  $^1\text{H NMR}$  (500 MHz,  $\text{CDCl}_3$ ):  $\delta$  (ppm) = 7.62 (s, 4H), 7.34 (dd,  $J=3.6$ , 1.2 Hz, 2H), 7.29 (dd,  $J=5.1$ , 1.1 Hz, 2H), 7.09 (dd,  $J=5.1$ , 3.6 Hz, 2H). GC-MS ( $m/z$ ) calcd for  $\text{C}_{14}\text{H}_{10}\text{S}_2$  [ $\text{M}^+$ ]: 242; Found 242.

**Synthesis of TPMe2.** The experimental steps are the same as TP. the mixture was concentrated and purified by column chromatography (silica, petroleum ether) afforded the title compound (870 mg, 85%) as a white solid.  $^1\text{H NMR}$  (500 MHz,  $\text{CDCl}_3$ ):  $\delta$  (ppm) = 7.35-7.34 (m, 2H), 7.33 (s, 2H), 7.11-7.09 (m, 4H), 2.42 (s, 6H); GC-MS ( $m/z$ ) calcd for  $\text{C}_{16}\text{H}_{14}\text{S}_2$  [ $\text{M}^+$ ]: 270; Found 270.

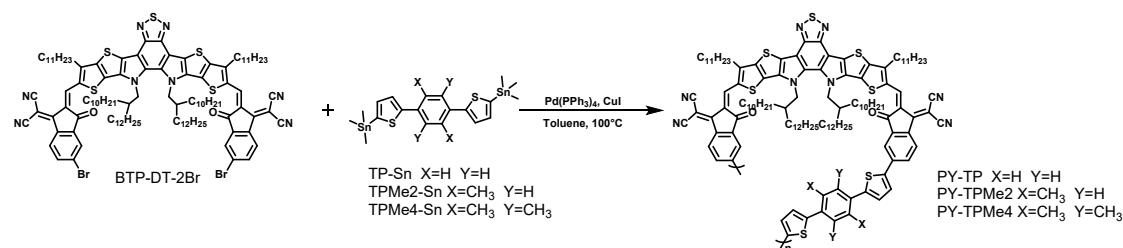
**Synthesis of TPMe4.** The experimental steps are the same as TP. The experimental steps are the same as TP. the mixture was concentrated and purified by column chromatography (silica, petroleum ether) afforded the title compound (839 mg, 82%) as a white solid.  $^1\text{H NMR}$  (500 MHz,  $\text{CDCl}_3$ ):  $\delta$  (ppm) = 7.38(dd,  $J = 5.2$ , 1.2 Hz, 2H), 7.12 (dd,  $J = 5.1$ , 3.4 Hz, 2H), 6.83(dd,  $J = 3.4$ , 1.2 Hz, 2H), 2.06 (s, 12H); GC-MS ( $m/z$ ) calcd for  $\text{C}_{18}\text{H}_{18}\text{S}_2$  [ $\text{M}^+$ ]: 294; Found 294.

**Synthesis of TP-Sn.** TP (500 mg, 2.06 mmol) and THF (15mL) were added into a 3-neck round bottom flask. Then Butyl lithium (n-BuLi) (2.5 M in hexane, 1.8 mL, 4.5 mmol) was added dropwise into solution stable at  $-78^\circ\text{C}$ . After stirring for 1h at  $-78^\circ\text{C}$  and 1 h at room temperature, the reaction was re-cooled to  $-78^\circ\text{C}$ , and dimethyltin chloride (897 mg, 4.5mmol) was added into the reaction system. Then it was stirred for 1h at  $-78^\circ\text{C}$  and for 12h at room temperature. The reaction system was quenched with cold potassium fluoride solution, extracted with diethyl ether, then dried and concentrated. After recrystallization of crude products in diethyl ether, white crystals were obtained (937mg, 80%).  $^1\text{H NMR}$  (500 MHz,  $\text{CDCl}_3$ ):  $\delta$  (ppm) = 7.61 (s, 4H), 7.44 (d,  $J=3.2\text{Hz}$ , 2H), 7.17 (d,  $J=3.3\text{Hz}$ , 2H), 0.40 (s, 18H).

**Synthesis of TPMe2-Sn.** The experimental steps are the same as TP-Sn. After recrystallization of crude products in diethyl ether, white crystals were obtained (920 mg, 75 %).  $^1\text{H NMR}$  (500 MHz,  $\text{CDCl}_3$ ):  $\delta$  (ppm) = 7.33 (s, 2H), 7.22 (d,  $J=3.2\text{Hz}$ , 2H), 7.18 (d,  $J=3.3\text{Hz}$ , 2H), 2.42 (s, 6H), 0.40 (s, 18H).

**Synthesis of TPMe4-Sn.** The experimental steps are the same as TP-Sn. After recrystallization of crude products in diethyl ether, white crystals were obtained (940 mg, 82 %). <sup>1</sup>H NMR (500 MHz, CDCl<sub>3</sub>): δ (ppm) = 7.18 (d, J=3.1Hz, 2H), 6.93 (d, J=3.1Hz, 2H), 2.04 (s, 12H), 0.40 (s, 18H).

**Synthesis of BTP-DT-2Br.** BTP-DT (900 mg, 0.52 mmol), IC-γ-Br (313 mg, 1.15 mmol) and Toluene (30 mL) were added into a single-neck flask. When the raw materials were dissolved in the solvent, acetic anhydride (0.24mL) and boron trifluoride etherate (0.37 mL) were added dropwise into solution separately. After stirring for 30min at room temperature, the reaction solution was dropped into 100mL Methanol sedimentation, then filter to collect the residue, which was purified by column chromatography (silica, petroleum ether: dichloroethane=3:1) afforded the title compound (930 mg, 90%) as a blue-black solid. <sup>1</sup>H NMR(500 MHz, CDCl<sub>3</sub>): δ (ppm) = 9.20 (s, 2H), 8.59 (d, J = 8.4 Hz, 2H), 8.04 (s, 2H), 7.88 (d, J = 10.4 Hz, 2H), 4.76 (d, J = 7.8 Hz, 4H), 3.24 (t, J = 8.0 Hz, 4H), 2.13-2.09 (m, 2H), 1.92-1.86 (m, 4H), 1.55-1.49 (m, 10H), 1.41-1.36 (m, 5H), 1.27-1.12 (m, 60H), 1.12-0.97 (m, 31H), 0.88-0.81 (m, 23H). <sup>13</sup>C NMR (500 MHz, CDCl<sub>3</sub>): δ (ppm) = 186.95, 159.96, 153.64, 147.51, 145.13, 138.52, 138.33, 137.68, 137.65, 135.92, 135.57, 134.19, 133.49, 130.83, 129.46, 126.71, 126.42, 120.13, 115.27, 114.91, 113.54, 68.30, 55.62, 39.13, 31.96, 31.93, 31.25, 30.53, 29.90, 29.85, 29.78, 29.71, 29.68, 29.64, 29.57, 29.56, 29.48, 29.41, 29.37, 29.35, 25.56, 22.72, 22.70, 14.13.



**Scheme S2** Synthetic routes of polymers.

### Synthesis of PY-TP, PY-TPMe2 and PY-TPMe4.

To a 10 mL Schlenk tube equipped with a stirring bar, TP-Sn (15 mg, 0.0258 mmol) and dibrominated monomer BTP-DT-2Br (80 mg, 0.0258 mmol), Pd (PPh<sub>3</sub>)<sub>4</sub> (1.18 mg, 1.29×10<sup>-3</sup> mmol), CuI (0.9 mg, 5.16×10<sup>-3</sup> mmol), and toluene (1.5 mL) were added.

The tube was purged with nitrogen and sealed under nitrogen flow and stirred at 100 °C for 2 hours. Then the reaction mixture was cooled down to room temperature and precipitated into 50 mL of methanol. The precipitate was filtrated, and then was extracted by Soxhlet extractor using CH<sub>3</sub>OH, acetone, n-hexane, and CHCl<sub>3</sub> successively. The CHCl<sub>3</sub> extraction was concentrated, re-precipitated into 50 mL methanol, filtrated, and dried to get the polymer (yield 68%): PY-TP (Mn=9.2 kDa, PDI=1.72)

To a 10 mL Schlenk tube equipped with a stirring bar, TPMe2-Sn (15.5 mg, 0.0258 mmol) and dibrominated monomer BTP-DT-2Br (80 mg, 0.0258 mmol), Pd (PPh<sub>3</sub>)<sub>4</sub> (1.18 mg, 1.29×10<sup>-3</sup> mmol), CuI (0.9 mg, 5.16×10<sup>-3</sup> mmol), and toluene (1.5 mL) were added. The tube was purged with nitrogen and sealed under nitrogen flow and stirred at 100 °C for 2 hours. Then the reaction mixture was cooled down to room temperature and precipitated into 50 mL of methanol. The precipitate was filtrated, and then was extracted by Soxhlet extractor using CH<sub>3</sub>OH, acetone, n-hexane, and CHCl<sub>3</sub> successively. The CHCl<sub>3</sub> extraction was concentrated, re-precipitated into 50 mL methanol, filtrated, and dried to get the polymer (yield 63%): PY-TPMe2 (GPC: Mn=8.8 kDa, PDI=1.92).

To a 10 mL Schlenk tube equipped with a stirring bar, TPMe4-Sn (16 mg, 0.0258 mmol) and dibrominated monomer BTP-DT-2Br (80 mg, 0.0258 mmol), Pd (PPh<sub>3</sub>)<sub>4</sub> (1.18 mg, 1.29×10<sup>-3</sup> mmol), CuI (0.9 mg, 5.16×10<sup>-3</sup> mmol), and toluene (1.5 mL) were added. The tube was purged with nitrogen and sealed under nitrogen flow and stirred at 100 °C for 2 hours. Then the reaction mixture was cooled down to room temperature and precipitated into 50 mL of methanol. The precipitate was filtrated, and then was extracted by Soxhlet extractor using CH<sub>3</sub>OH, acetone, n-hexane, and CHCl<sub>3</sub> successively. The CHCl<sub>3</sub> extraction was concentrated, re-precipitated into 50 mL methanol, filtrated, and dried to get the polymer (yield 65%): PY-TPMe4 (GPC: Mn=9.1 kDa, PDI=1.78).

## **1.2. General information for measurements and characterizations**

The <sup>1</sup>H NMR and <sup>13</sup>C NMR spectra were recorded on a Bruker AV-500 spectrometer. The mass spectra were measured by a Bruker AutoflexIII smartbeam MALDI-TOF

mass spectrometer (MALDI-TOF MS). DFT calculations were conducted by using the Gaussian 09 software package at the B3LYP/6-31G(d) level. Thermogravimetric analysis (TGA) was performed under nitrogen flow at a heating rate of 10 °C min<sup>-1</sup> on a TA-TGA55, and the temperature of degradation ( $T_d$ ) corresponds to 5% mass loss. UV-vis absorption spectra were measured on a PerkinElmer Lambda 35 UV-vis spectrometer. Photoluminescence (PL) spectra were measured on a FluoroLog-3 spectrofluorometer. Cyclic voltammetry (CV) measurements were performed on a CHI660a electrochemical workstation with a glassy carbon working electrode, a platinum counter electrode, and a saturated calomel reference electrode. Tetra-*n*-butylammonium perchlorate (*n*-Bu<sub>4</sub>NClO<sub>4</sub>) in acetonitrile solution with a concentration of 0.1 M was used as the supporting electrolyte. Ferrocene was used as the reference, and the potential of its redox couple (Fc/Fc<sup>+</sup>) is assumed to be 4.8 eV below the vacuum level. The materials were casted on the working electrode for measurements, and all CV measurements were performed with a scan rate of 50 mV s<sup>-1</sup>. The thickness of the blend films was measured with a KLA-Tencor profiler P-7. Atomic force microscopy (AFM) images were measured with the SPI 3800N Probe Station and SPA-300HV unit system (Seiko Instruments Inc., Japan) in tapping mode. Grazing-incidence wide-angle X-ray scattering (GIWAXS) data were obtained at 1W1A Diffuse X-ray Scattering Station, Beijing Synchrotron Radiation Facility (BSRF-1W1A). The monochromatic of the light source was 1.54 Å. The data were recorded by using the two-dimensional image plate detector of Eiger 2M from Dectris, Switzerland. Crystal coherence length (CCL) was calculated according to the reported method.

### **1.3. Fabrication and measurement of OSC devices**

The organic solar cell devices were fabricated with the conventional structure of ITO/PEDOT:PSS/PM6:PY-TP series/PDNIT-F3N/Ag. The ITO-coated glass substrates were cleaned in an ultrasonic bath with isopropyl alcohol, deionized water, acetone, and isopropyl alcohol in sequence, and then drying at 120 °C for 30 min in an oven. After treated with ultraviolet-ozone for 30 min, PEDOT:PSS layer was spin-coated onto the ITO substrates at 5000 rpm for 40 s and then drying in an oven at 120 °C for 30 min. After that, the PEDOT:PSS-coated ITO substrates were transferred into

a nitrogen-filled glovebox quickly. Active layer solutions of PM6:PY-TP series (the D:A mass ratio is 1:1, and the total concentration is 12 mg/mL) in chloroform were spin-coated onto the PEDOT:PSS layer at 2500rpm to 3000rpm for 1 min to obtain the active layers with thickness of about 120 nm, respectively. After treated the active layer with thermal annealing at 120 °C for 10 min, PDNIT-F3N in methanol solution (1 mg mL<sup>-1</sup>) with 1%vt acetic acid was spin-coated onto the active layer at 3000 rpm for 30 s. Finally, a 100 nm Ag layer was deposited on the PDNIT-F3N layer by thermal evaporation under a pressure of about  $2 \times 10^{-4}$  Pa in a vacuum chamber. The active area of the devices was 8 mm<sup>2</sup>. The current density-voltage (*J-V*) curves of the devices were measured with a computer-controlled Keithley 2400 source meter. The 100mW cm<sup>-2</sup> AM 1.5G simulated solar light illumination was provided by a XES-40S2-CE class solar simulator (Japan, SAN-EI Electric Co., Ltd.). External quantum efficiency (EQE) spectra were measured with a solar cell spectral response measurement system QE-R3011 (Enlitech Co., Ltd.), which was calibrated by a certified standard monocrystalline silicon solar cell before use.

#### 1.4. Hole/electron mobility measurements

Charge mobilities of the blend films were measured by the space-charge-limited current (SCLC) method. The hole-only and electron-only devices were fabricated with the structures of ITO/PEDOT:PSS/PM6:PY-TP series/MoO<sub>3</sub>/Ag and ITO/ZnO/PM6:PY-TP series /PDNIT-F3N/Ag, respectively. The *J-V* curves were measured in the dark and the mobilities were determined by fitting the dark current to the model of a single carrier SCLC that expressed by the modified Mott-Gurney formula:  $J = 9\epsilon_r\epsilon_0\mu V^2\exp(0.89\beta(V/L)^{0.5})/8L^3$ . Where *J* is the current density,  $\epsilon_r$  is the relative permittivity of the transport materials (assumed to be 3),  $\epsilon_0$  is the permittivity of free space ( $8.85 \times 10^{-12}$  F m<sup>-1</sup>),  $\mu$  is the charge mobility, *V* is the effective voltage ( $V = V_{\text{appl}} - V_{\text{bi}}$ ,  $V_{\text{appl}}$  is the applied voltage and  $V_{\text{bi}}$  is the built-in voltage due to the relative work function difference of the two electrodes),  $\beta$  is the field-activation factor, and *L* is the thickness of the blend films.

## 2. Figures and tables section

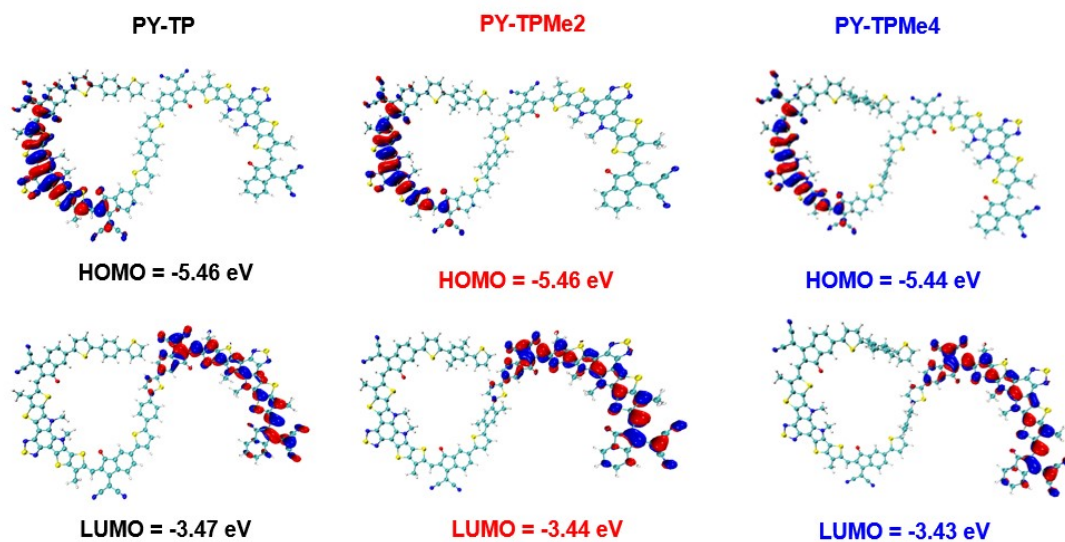


**Fig. S1** The frontier molecular orbitals of PY-TP, PY-TPMe2 and PY-TPMe4 calculated by a DFT method at the B3LYP/6-31G(d, p) set.

**Table S1** The parameters of PY-TP, PY-TPMe2 and PY-TPMe4 calculated by a DFT method at the B3LYP/6-31G(d,p) set.

	$E_{\text{HOMO}}$ (eV)	$E_{\text{LUMO}}$ (eV)	$E_{\text{g}}^{\text{opt}}$ (eV)	$S_1$	$T_1$	$f_{S_1}$
PY-TP	-5.46	-3.47	1.99	1.75	1.27	2.29
PY-TPMe2	-5.46	-3.44	2.02	1.78	1.27	2.66
PY-TPMe4	-5.44	-3.43	2.01	1.81	1.27	2.22

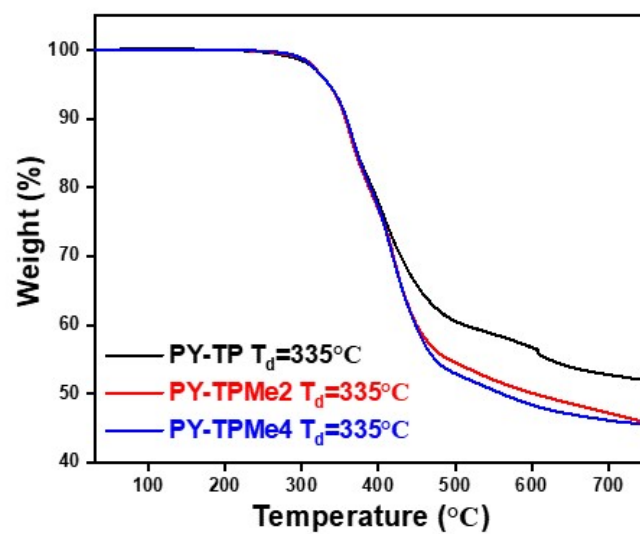


**Fig. S2** TGA measurements of PY-TP, PY-TPMe2 and PY-TPMe4.

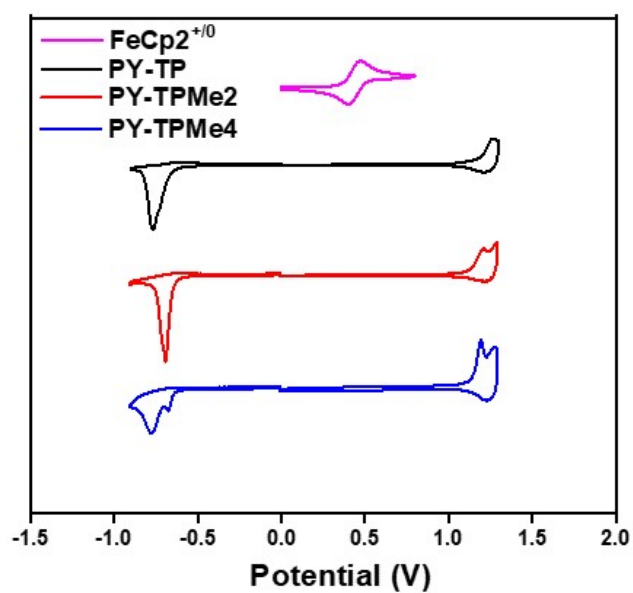


**Fig. S3** Cyclic voltammograms of PM6, PY-TP, PY-TPMe2 and PY-TPMe4.

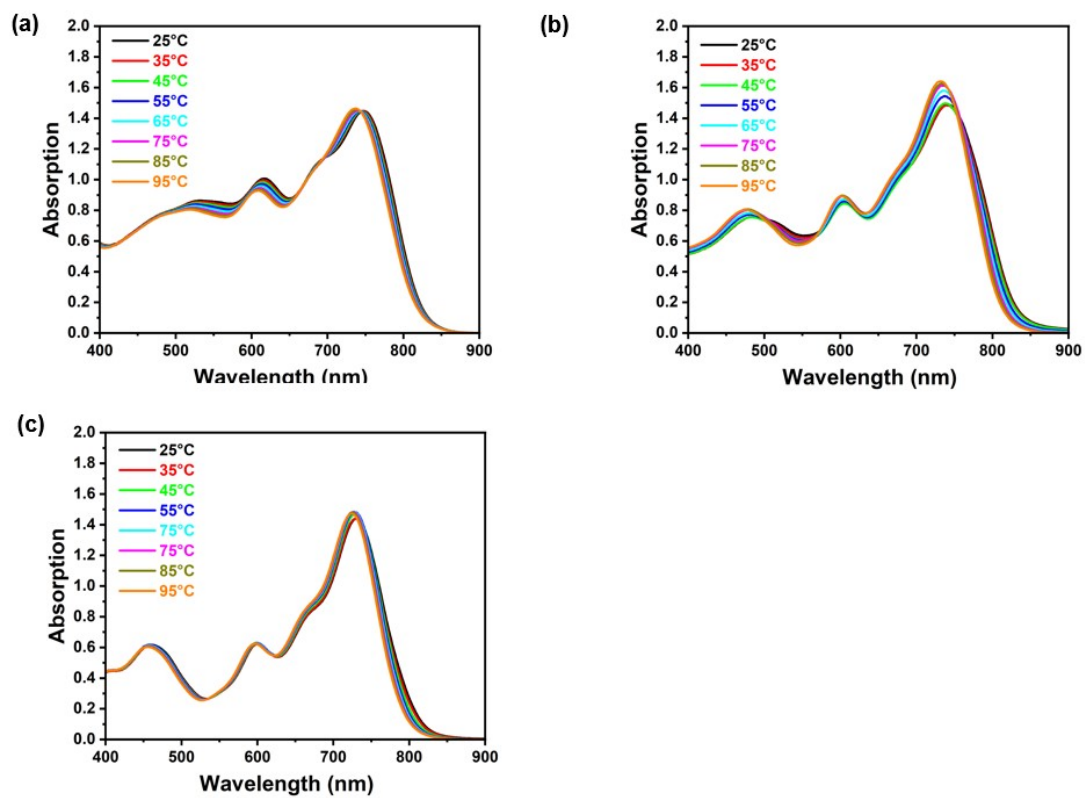


**Fig. S4** Temperature-dependent absorption spectra of (a) PY-TP, (b) PY-TPMe<sub>2</sub>, and (c) PY-TPMe<sub>4</sub> in chlorobenzene solutions.

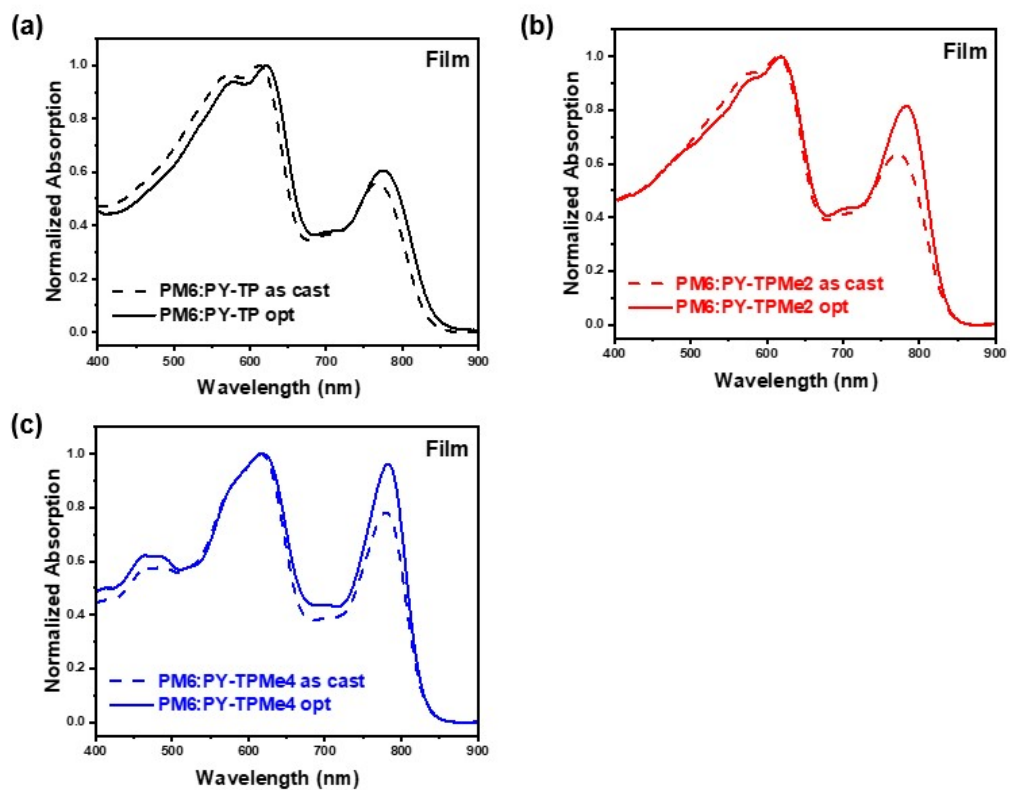


**Fig. S5** Absorption spectra of (a) as cast PM6:PY-TP and optimized PM6:PY-TP blend films, (b) as cast PM6:PY-TPMe2 and optimized PM6:PY-TPMe2 blend films, (c) as cast PM6:PY-TPMe4 and optimized PM6:PY-TPMe4 blend films.

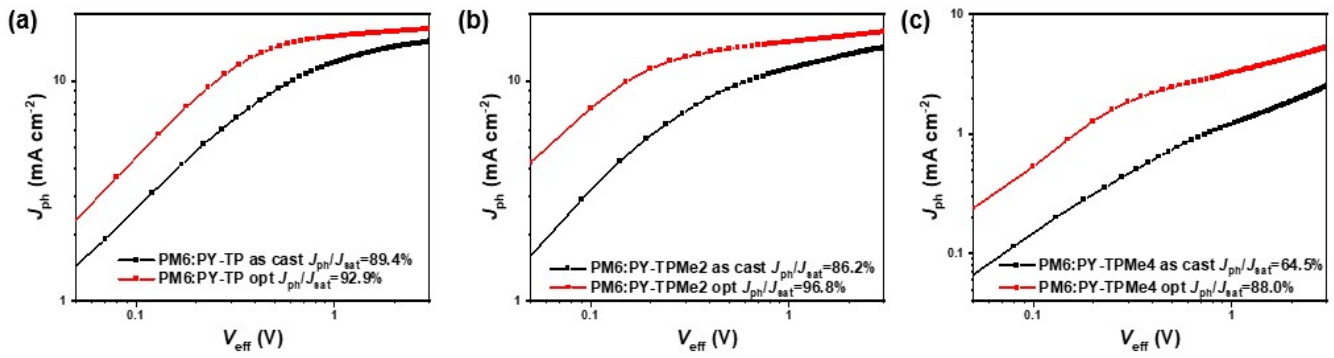


**Fig. S6**  $J_{ph}$  versus  $V_{eff}$  versus light intensity characteristics of OSC devices based on (a) as cast and optimized PM6: PY-TP blends, (b) as cast and optimized PM6: PY-TPMe2 blends and (c) as cast and optimized PM6: PY-TPMe4 blends.

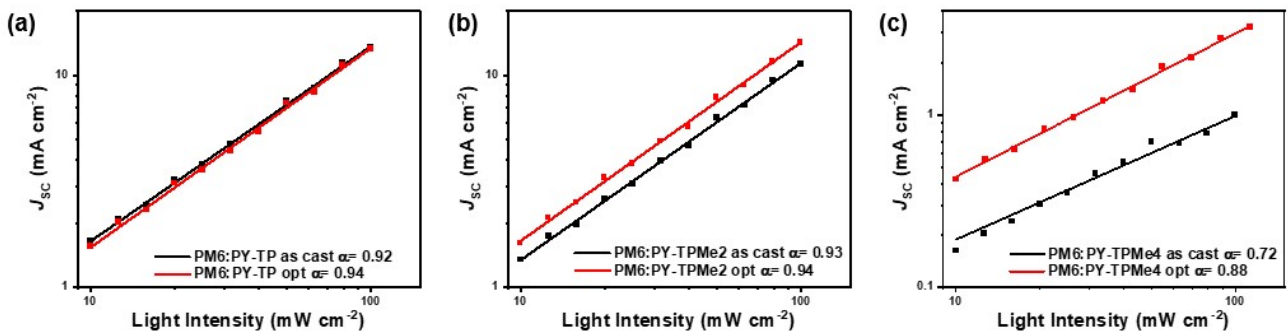


**Fig. S7**  $J_{sc}$  versus light intensity characteristics of OSC devices based on (a) as cast and optimized PM6: PY-TP blends, (b) as cast and optimized PM6: PY-TPMe2 blends and (c) as cast and optimized PM6: PY-TPMe4 blends.

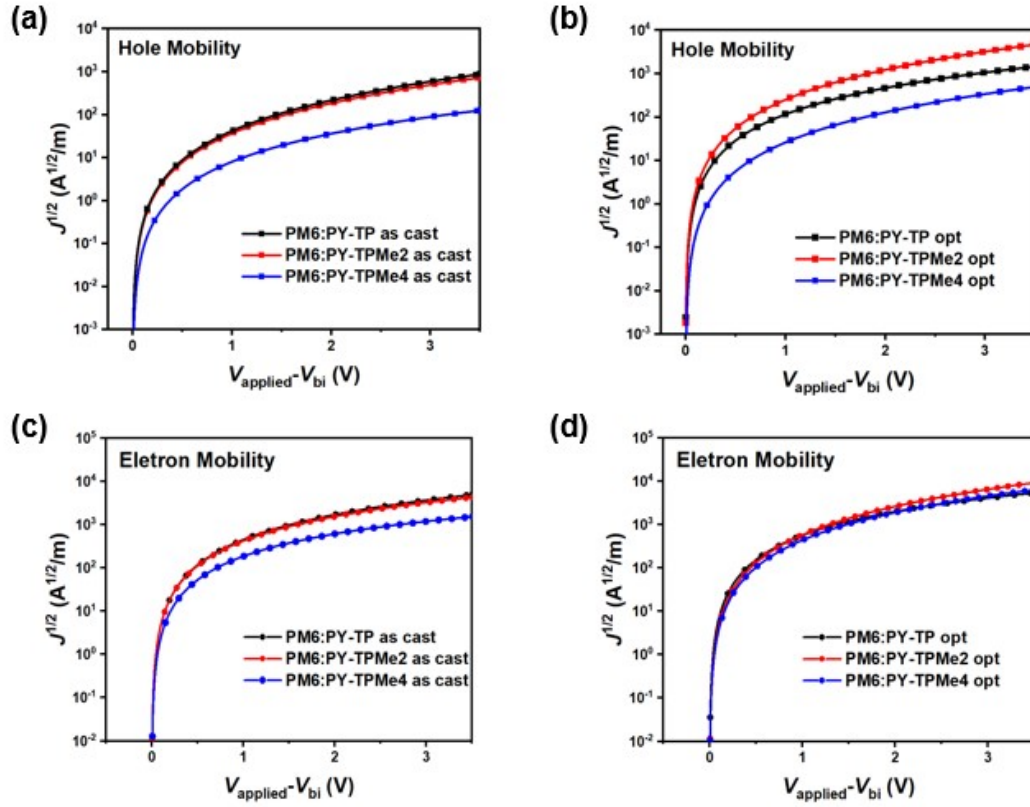


**Fig. S8**  $J^{1/2}$ - $V$  characteristics were acquired from (a) Hole-Mobility and (b) Electron-Mobility devices based on as cast and optimized PM6: PY-TP, PM6: PY-TPMe2 and PM6: PY-TPMe4 blends.

**Table S2.** Hole and electron mobilities of six PM6: acceptor blends.

Active layer		$\mu_h$ ( $\text{cm}^2 \text{v}^{-1}\text{s}^{-1}$ )	$\mu_e$ ( $\text{cm}^2 \text{v}^{-1}\text{s}^{-1}$ )
PM6:PY-TP	as cast	$2.78 \times 10^{-5}$	$4.18 \times 10^{-4}$
	optimized	$6.42 \times 10^{-5}$	$4.36 \times 10^{-4}$
PM6:PY-TPMe2	as cast	$2.57 \times 10^{-5}$	$4.29 \times 10^{-4}$
	optimized	$1.26 \times 10^{-4}$	$5.82 \times 10^{-4}$
PM6:PY-TPMe4	as cast	$4.88 \times 10^{-6}$	$2.42 \times 10^{-4}$
	optimized	$1.28 \times 10^{-5}$	$2.96 \times 10^{-4}$

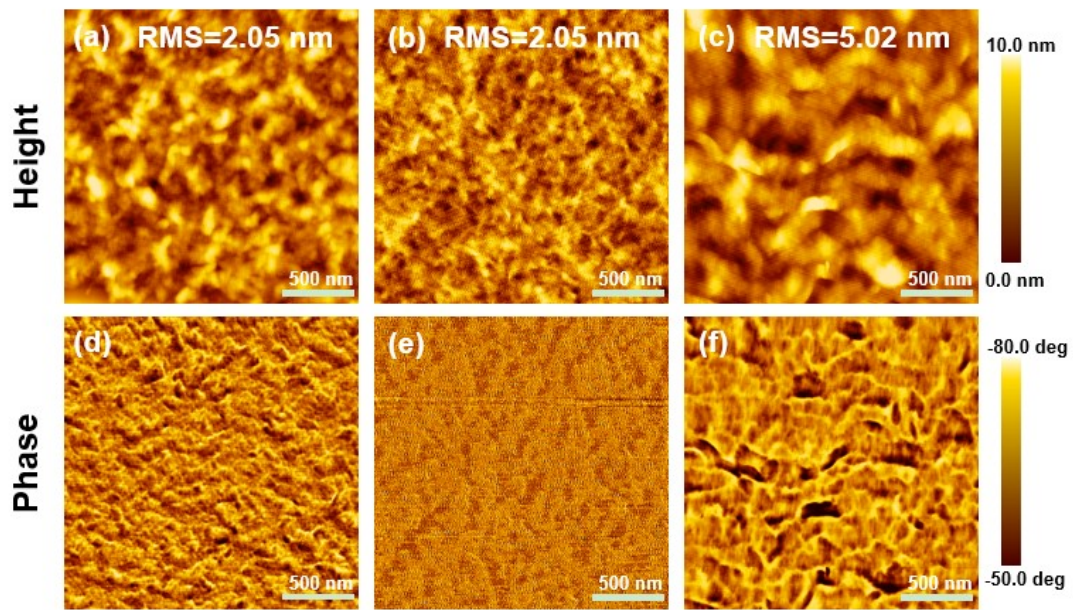


**Fig. S9** AFM height images of (a) PY-TP, (b) PY-TPMe2 and (c) PY-TPMe4 neat films; AFM phase images of (d) PY-TP, (e) PY-TPMe2 and (f) PY-TPMe4 neat films.

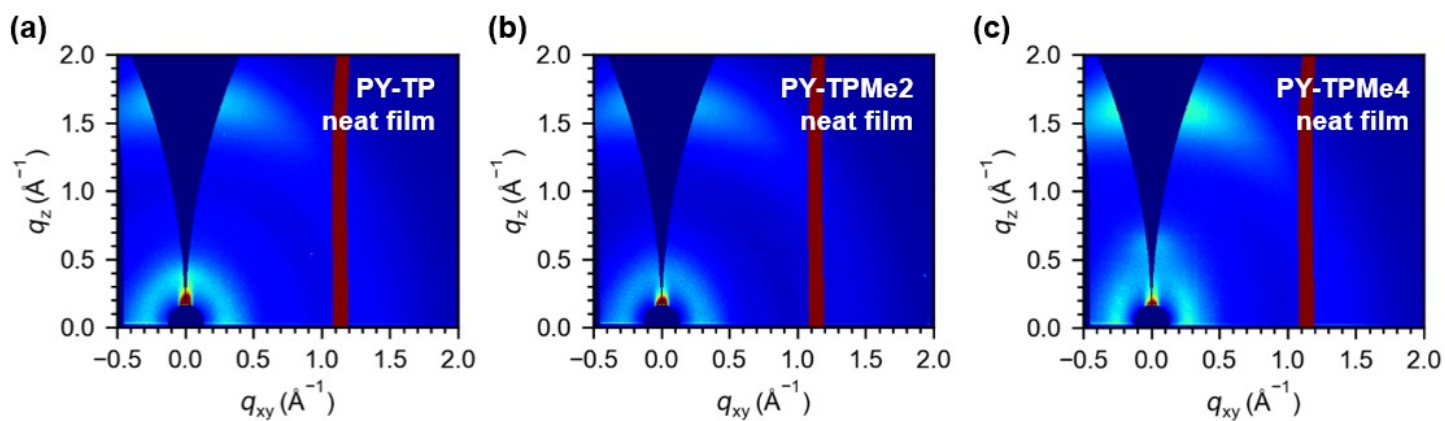


**Fig. S10** (a-c) 2D-GIWAXS patterns among IP and OOP directions of PY-TP, PY-TPMe2 and PY-TPMe4 neat film.

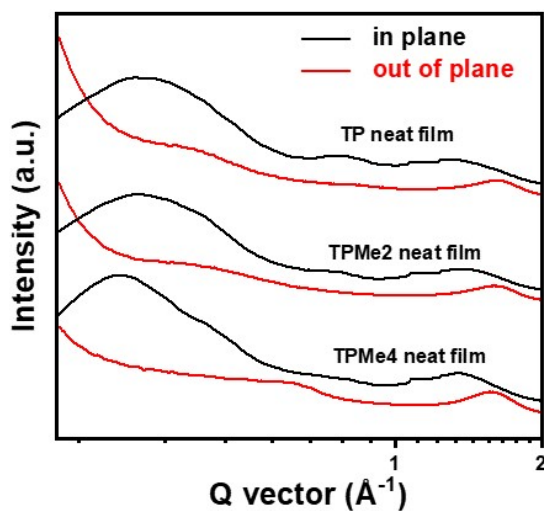


**Fig. S11** 2D-GIWAXS line-cut profiles among IP and OOP directions of PM6:PY-TP, PY-TPMe2 and PY-TPMe4 neat film.

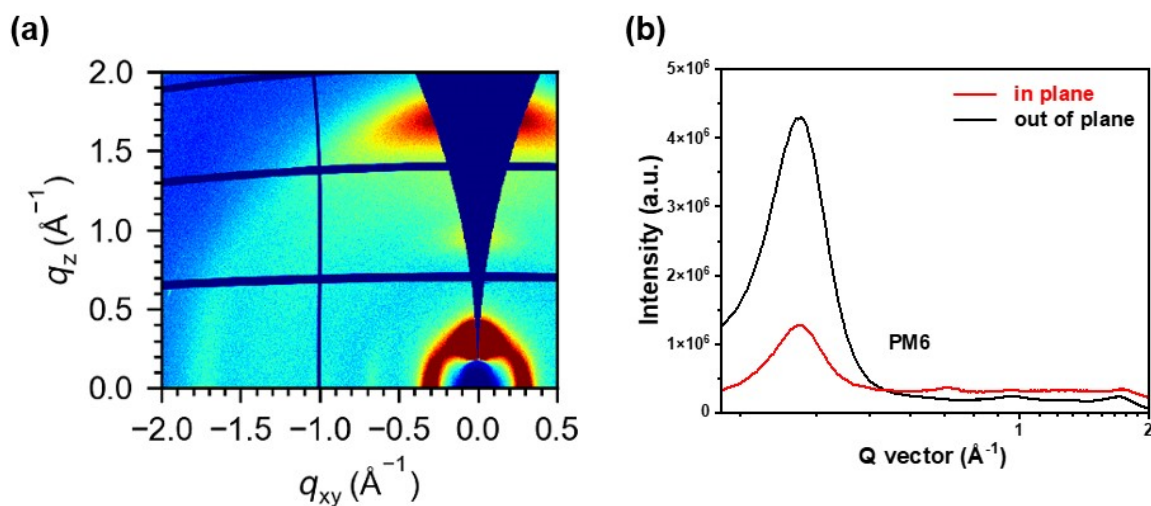


**Figure S12.** (a) 2D-GIWAXS patterns and (b) line-cut profiles among IP and OOP directions of PM6 neat film.

**Table S3.** The detailed GIWAXS data of neat acceptors films.

Neat film	In plane			Out of plane					
	(100) peaks			(100) peaks			(010) peaks		
	$q_z$ ( $\text{\AA}^{-1}$ )	d-spacing ( $\text{\AA}$ )	CCL ( $\text{\AA}$ )	$q_z$ ( $\text{\AA}^{-1}$ )	d-spacing ( $\text{\AA}$ )	CCL ( $\text{\AA}$ )	$q_z$ ( $\text{\AA}^{-1}$ )	d-spacing ( $\text{\AA}$ )	CCL ( $\text{\AA}$ )
TP	0.29	21.44	28.4	-	-	-	1.64	3.84	15.2
TPMe2	0.29	21.67	28.4	-	-	-	1.60	3.92	14.9
TPMe4	0.27	23.27	38.2	-	-	-	1.59	3.96	15.9
PM6	0.31	20.60	65.0	0.31	20.53	57.7	1.71	3.67	19.0

**Table S4.** The detailed GIWAXS data of PM6: acceptors blend films.

Blend Film		In plane			Out of plane					
		(100) peaks			(100) peaks			(010) peaks		
		$q_z$ ( $\text{\AA}^{-1}$ )	d-spacing ( $\text{\AA}$ )	CCL ( $\text{\AA}$ )	$q_z$ ( $\text{\AA}^{-1}$ )	d-spacing ( $\text{\AA}$ )	CCL ( $\text{\AA}$ )	$q_z$ ( $\text{\AA}^{-1}$ )	d-spacing ( $\text{\AA}$ )	CCL ( $\text{\AA}$ )
PM6:PY-TP	as cast	0.30	21.29	47.1	0.33	19.15	50.5	1.64	3.83	16.6
	optim	0.30	20.93	72.5	0.32	19.94	83.2	1.67	3.76	18.9
PM6: PY-TPME2	as cast	0.29	22.04	47.1	0.32	19.75	53.4	1.64	3.84	16.5
	optim	0.30	21.07	68.9	0.31	20.06	72.5	1.65	3.80	17.1
PM6: PY-TPME4	as cast	0.29	21.66	47.5	0.33	19.15	64.9	1.62	3.88	16.6
	optim	0.30	21.29	69.8	0.32	19.75	80.8	1.64	3.84	16.0

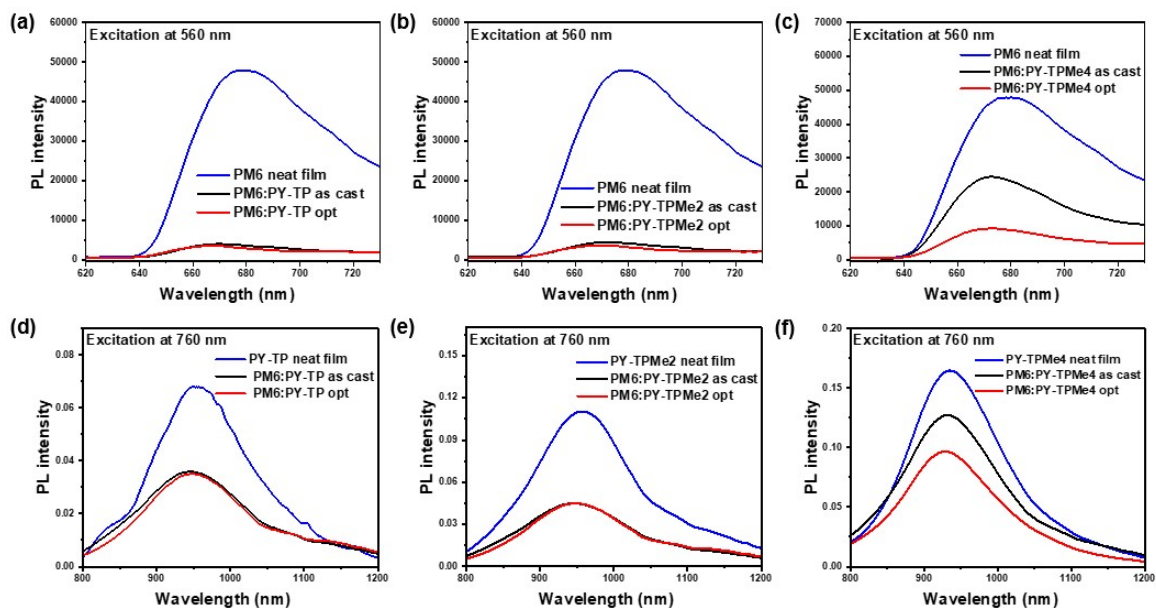


**Fig. S13** (a-c) PL spectra of PM6 neat film and PM6:acceptors blend films. (d) PL spectra of PY-TP neat film and PM6:PY-TP blend films. (e) PL spectra of PY-TPMe2 neat film and PM6: PY-TPMe2 blend films. (f) PL spectra of PY-TPMe4 neat film and PM6: PY-TPMe4 blend films.

Active layer	PM6: PY-TP		PM6: PY-TPMe2		PM6: PY-TPMe4	
	as cast	optimized	as cast	optimized	as cast	optimized
acceptors	46%	49%	59%	60%	23%	42%
doner	91%	93%	91%	93%	49%	81%

**Table S5.** The PL spectra data of PM6: acceptors blend films.

**Table S6.** Photovoltaic performance of PM6:PY-TPMe2-based OSC devices under different D/A.

Doner: Acceptor	D/A	V <sub>oc</sub> (V)	J <sub>sc</sub> (mA cm <sup>-2</sup> )	FF (%)	PCE (%)
PM6: PY-TPMe2 with 1%PN 120°CCTA	1: 0.6	0.97	13.92	0.47	6.35
	1:0.8	0.97	13.3	0.54	7.06
	1:1	0.96	15.35	0.55	8.11
	1:1.2	0.96	14.09	0.47	7.37

**Table S7.** Photovoltaic performance of PM6:PY-TPMe2-based OSC devices under different processing.

Doner: Acceptor	processing	V <sub>oc</sub> (V)	J <sub>sc</sub> (mA cm <sup>-2</sup> )	FF (%)	PCE (%)
PM6: PY-TPMe2 1: 1 12mg/mL	ascast	0.98	11.37	0.48	5.33
	1%PN 100°CCTA	0.98	14.15	0.60	8.32
	0.5%PN 120°CCTA	0.97	14.19	0.56	7.66
	1%PN 120°CCTA	0.97	14.74	0.59	8.43
	2%PN 120°CCTA	0.97	13.93	0.59	7.91
	1%PN 140°CCTA	0.97	14.23	0.60	8.23

**Table S8.** Photovoltaic performance of PM6:PY-TP-based OSC devices under different D/A.

Doner: Acceptor	D/A	V <sub>oc</sub> (V)	J <sub>sc</sub> (mA cm <sup>-2</sup> )	FF (%)	PCE (%)
PM6: PY-TP with 1%PN 120°CCTA	1:0.8	0.89	14.49	0.46	5.96
	1:1	0.87	15.34	0.50	6.69
	1:1.2	0.87	13.56	0.49	5.82

**Table S9.** Photovoltaic performance of PM6:PY-TP-based OSC devices under different processing.

Doner: Acceptor	processing	V <sub>oc</sub> (V)	J <sub>sc</sub> (mA cm <sup>-2</sup> )	FF (%)	PCE (%)
PM6: PY-TP 1: 1 12mg/mL	ascast	0.97	12.80	0.43	5.34
	1%PN 100°CCTA	0.86	14.44	0.52	6.43
	1%PN 120°CCTA	0.87	15.34	0.50	6.69
	1%PN 140°CCTA	0.88	15.35	0.51	6.9
	1%PN 160°CCTA	0.86	14.70	0.52	6.52
	0.5%PN 140°CCTA	0.87	11.84	0.56	5.77
	2%PN 140°CCTA	0.84	15.07	0.50	6.30

**Table S10.** Photovoltaic performance of PM6:PY-TPMe4-based OSC devices under different processing.

Doner: Acceptor	processing	V <sub>oc</sub> (V)	J <sub>sc</sub> (mA cm <sup>-2</sup> )	FF (%)	PCE (%)
PM6: PY-TPMe4 1: 1 12mg/mL	ascast	0.98	1.02	0.36	0.36
	1%PN 80°CCTA	0.97	2.80	0.40	1.09
	1%PN 100°CCTA	0.97	2.98	0.40	1.17
	1%PN 120°CCTA	0.98	3.37	0.42	1.37
	1%PN 140°CCTA	0.97	3.20	0.38	1.30

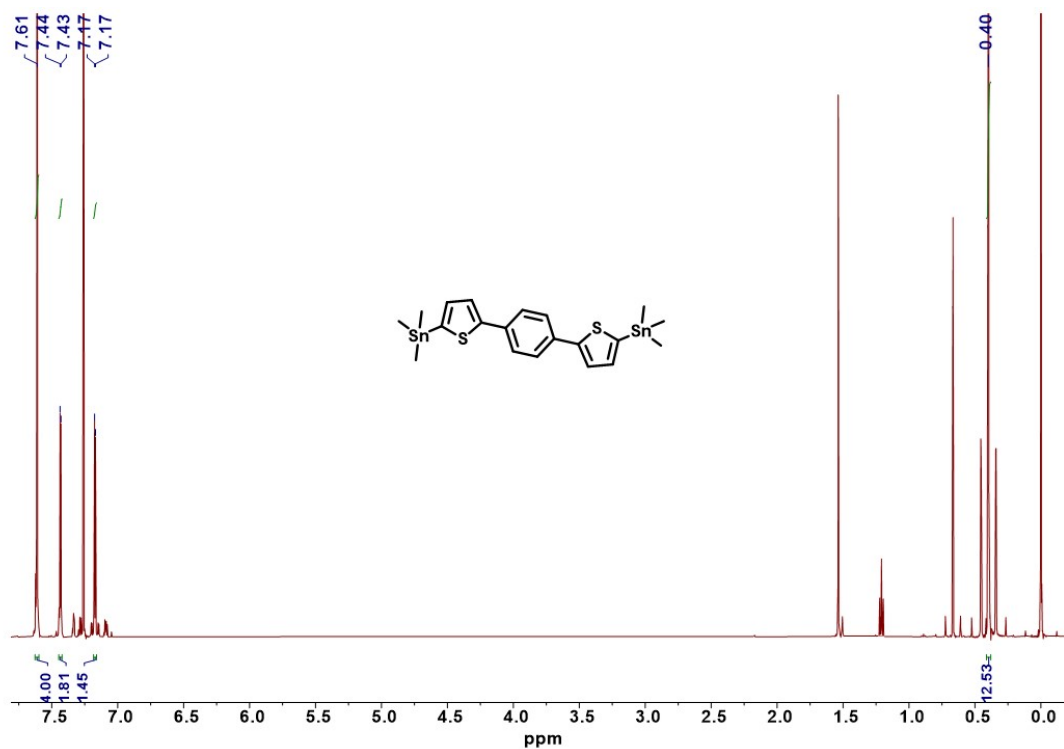


Figure S14 The  $^1\text{H}$  NMR spectrum of compound TP-Sn.

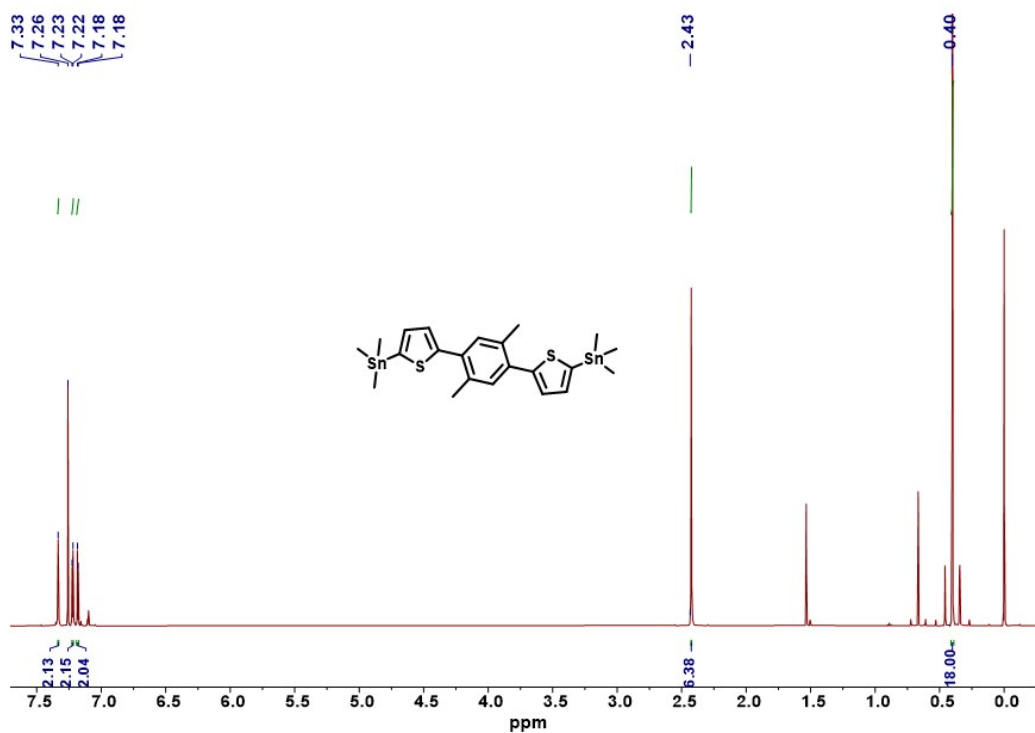


Figure S15 The  $^1\text{H}$  NMR spectrum of compound TPMe<sub>2</sub>-Sn.

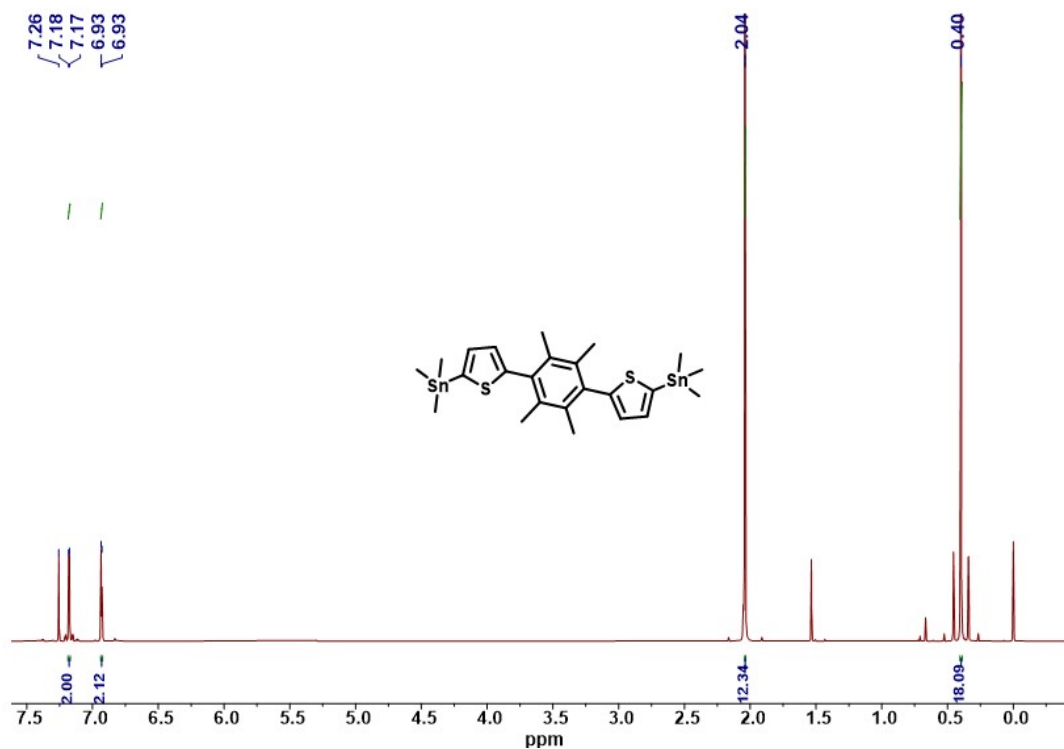


Figure S16 The  $^1\text{H}$  NMR spectrum of compound TPMe4-Sn.

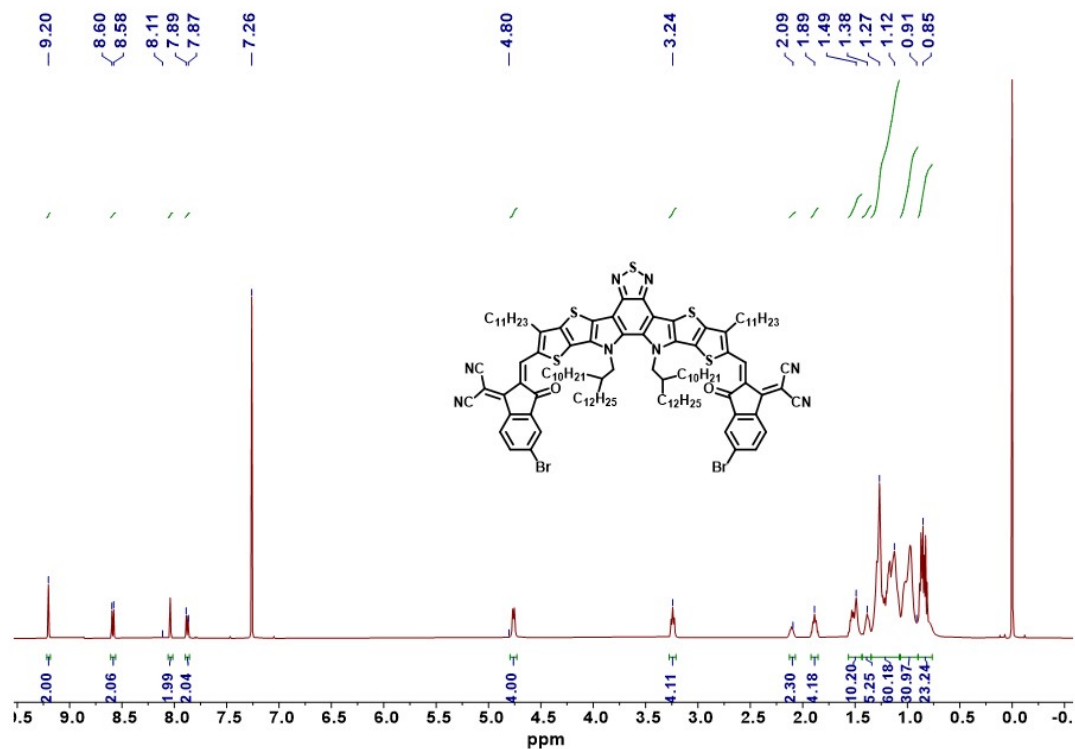


Figure S17 The  $^1\text{H}$  NMR spectrum of BTP-DT-2Br.

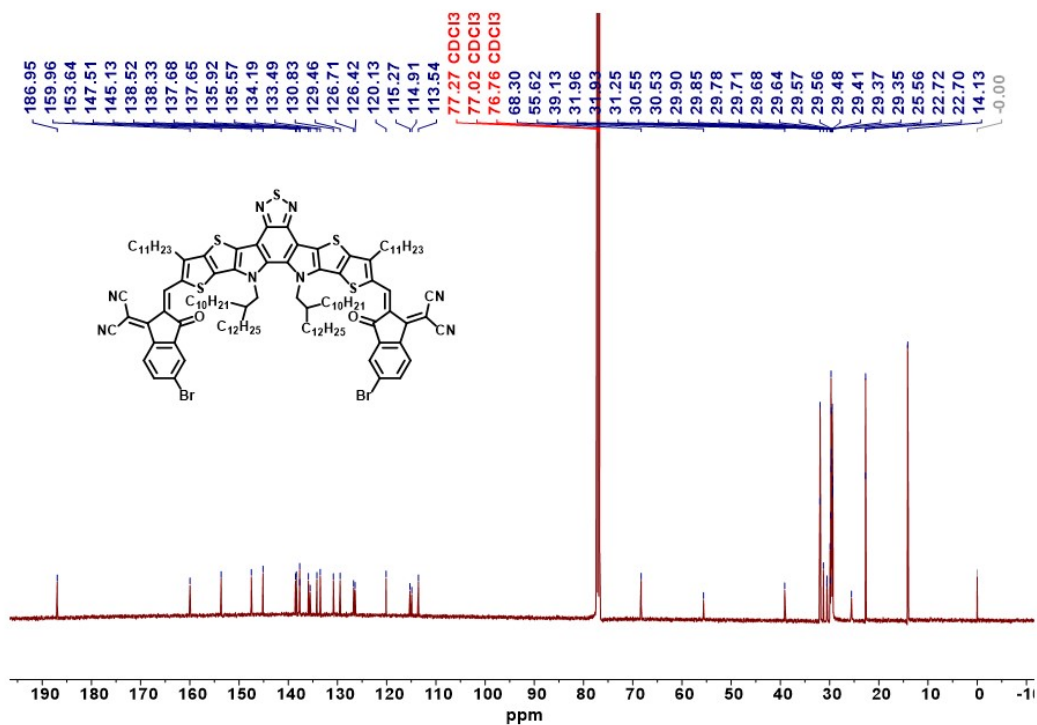


Figure S18 The <sup>13</sup>C NMR spectrum of BTP-DT-2Br.

Comment 1  
Comment 2

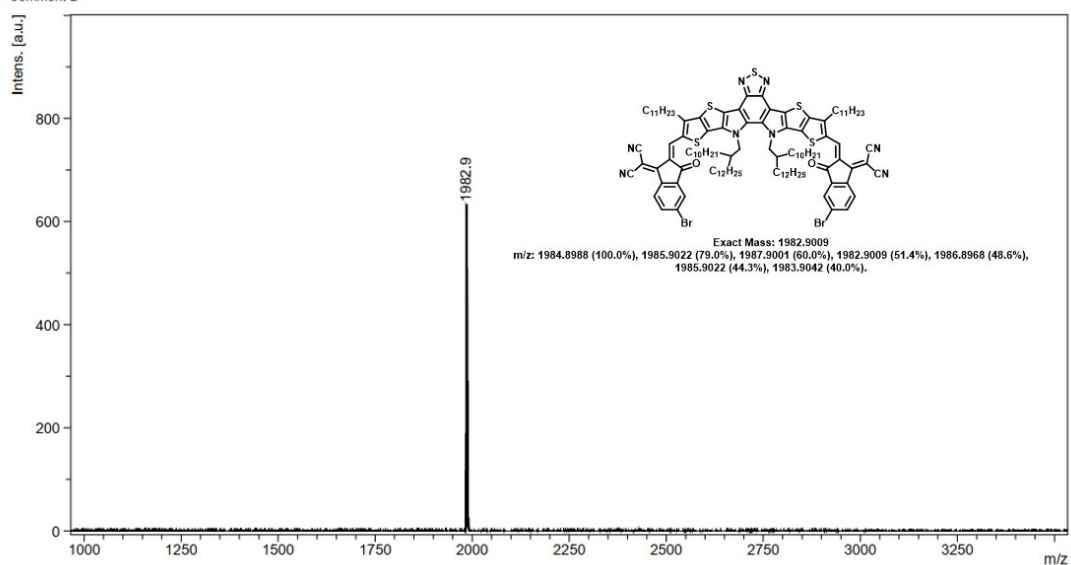
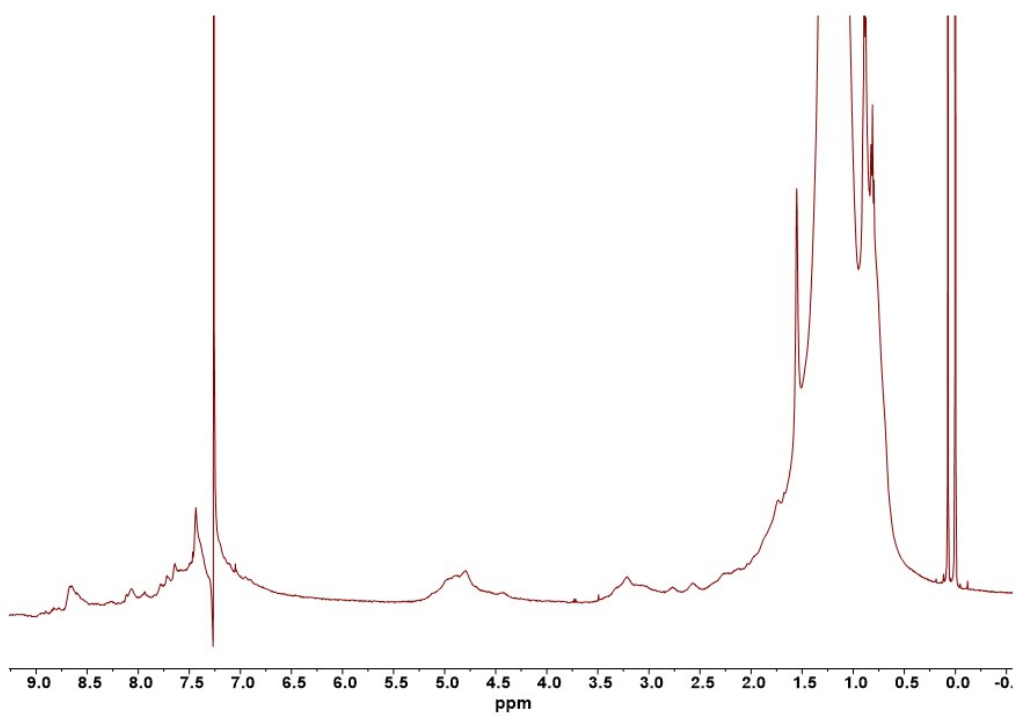
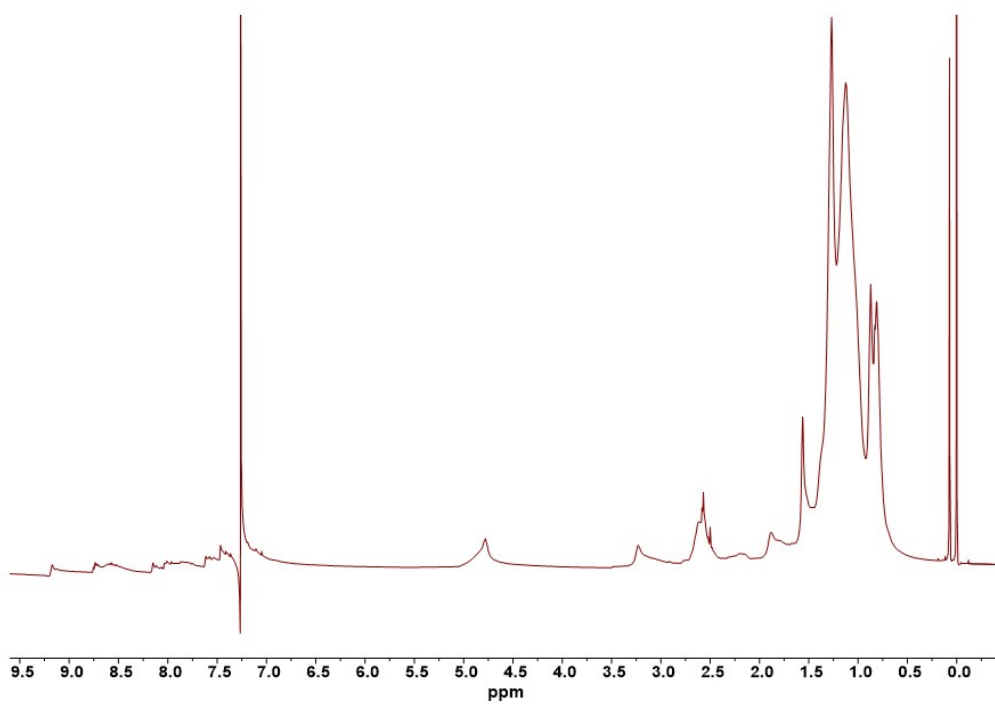


Figure S19 The MALDI-TOF high resolution mass spectrum of BTP-DT-2Br.



**Figure S20** The <sup>1</sup>H NMR spectrum of PY-TP.



**Figure S21** The <sup>1</sup>H NMR spectrum of PY-TPMe<sub>2</sub>.

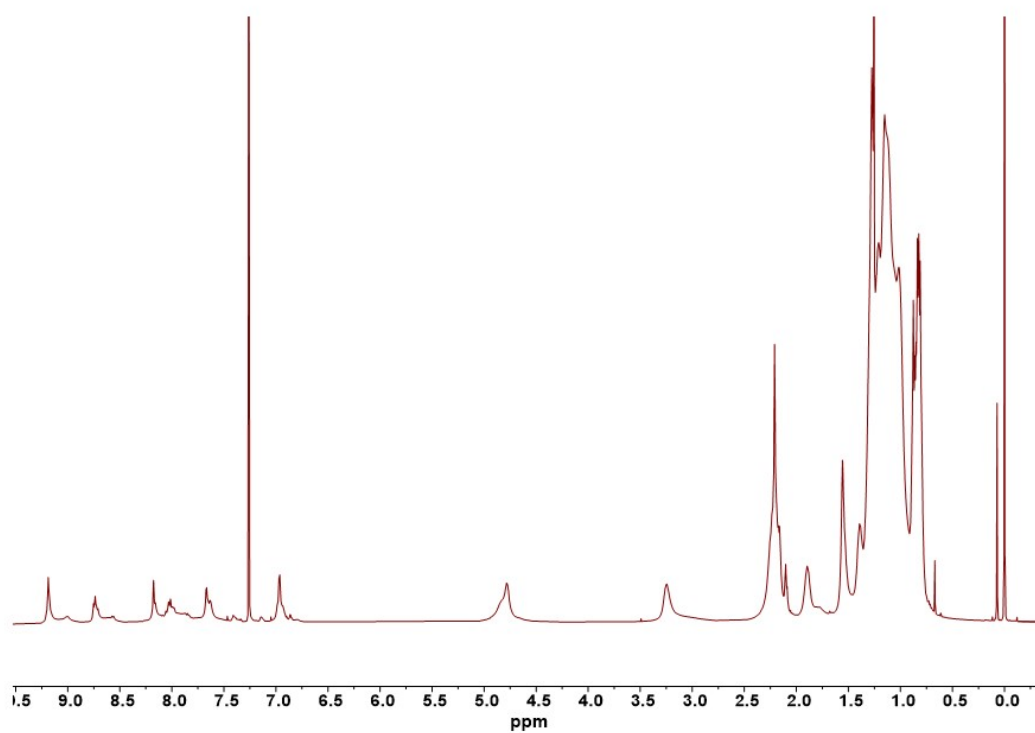


**Figure S22** The  $^1\text{H}$  NMR spectrum of **PY-TPMe4**.